ACI STRUCTURAL JOURNAL TECHNICAL PAPER

Title no. 93-S24

Stress Transfer Mechanism of Socket Base Connections With Precast Concrete Columns



by Yutaka Osanai, Fumio Watanabe, and Shin Okamoto

The purpose of this study is to derive a rational design method and connection details for socket base column-to-foundation connections for earthquake-resistant buildings. Cyclic loading tests on one-half-scale model specimens were conducted to investigate the structural behavior of socket base connections. From experimental observations, modeling of the resultant force transfer mechanism of socket base connections was also carried out. Finally, a practical design method of connection details for socket base connections was proposed using the aforementioned model.

Keywords: columns (supports); earthquake-resistant structures; joints (junctions); models; precast concrete.

INTRODUCTION

Bases of reinforced concrete columns that provide connections in precast structural systems are generally pressed onto or embedded in foundations or encased with concrete. Of these types of column base connections, embedded columns provide the simplest form, one that has been used in wooden structures since ancient times.

There are no standards in Japan for the design of embedded column base connections constructed with reinforced concrete. The method used for practical purposes is the one given in the "Recommendations for the Design and Fabrication of Tubular Structures in Steel"[1] (hereafter referred to as AIJ Recom.), in which a design method to achieve the ultimate bending strength of embedded columns is given.

In Germany, on the other hand, calculation methods for the steel sectional area required for reinforcement of embedded column base foundations are specified in DIN 1045.[2] In this method, the equations used for the calculations are selected according to the conditions of the interface between column faces and the internal faces of the sockets.

Test results obtained by the authors indicated that AIJ Recom. and DIN 1045 are too conservative. The reason is that in these two methods interface frictions and the bottom reaction are not properly evaluated.

This study proposes an equation for the calculation of the resultant force in the embedded portions, taking into account the column axial forces and the friction forces generated between the precast column bases and internal faces of the sockets. The validity of this theoretical equation was verified through comparison with results obtained from model tests.

Theoretical approach

Analysis on socket base of perimeter column—Precast concrete columns are erected according to the following procedure. A socket is first created in the reinforced concrete foundation. The precast concrete column is then inserted into the socket and set in position. Finally, the space between the column and the socket walls is filled with concrete to achieve a rigid connection between the foundation and the column. This method allows the adjustment of the column position even after the hardening of the foundation concrete. It is also a useful method in which the strength of the column bases can be calculated with ease from specifications using a simple equilibrium model.

Regarding socket bases, there is no report about the accurate transfer mechanism of the force at the column foot or the combination of the forces in the socket base and the calculating method of the force magnitude except DIN 1045.

When the column axial force and horizontal force act on the column, overturning moment and shear force are generated at the column foot. These forces result in horizontal reactions, interface frictions, and bottom reaction. The realistic equilibrium condition of an embedded column is illustrated in Fig. 1. However, in the AIJ Recom. only the horizontal reactions C and C_{22} are counted. That is, the interface frictions F_1, F_2, and F_3 and bottom reaction R, due to column axial force, are not counted.

The total model (Fig. 2) on which these forces act can be divided into Model 1 (Fig. 3) and Model 2 (Fig. 4). Model 1 is the case in which loads are resisted by horizontal reaction force and axial force, and Model 2 is the case in which loads are resisted by horizontal reaction forces and friction forces.

ACI Structural Journal, V. 93, No. 3, May-June 1996.
Received May 27, 1994, and reviewed under Institute publication policies. Pertinent discussion will be published in the March-April 1997 *ACI Structural Journal* if received by Nov. 1, 1996.

Yutaka Osanai *is a senior research engineer at Oriental Construction Co., Ltd., Tokyo, Japan. He received his master's degree from Kumamoto University in 1977. He is a member of the Japan Concrete Institute and the Architectural Institute of Japan. His research interests include seismic design of reinforced concrete, prestressed concrete, and precast concrete buildings.*

ACI member ***Fumio Watanabe*** *is a professor at Kyoto University, Kyoto, Japan. He received his doctorate degree from Kyoto University in 1984. He is a member of the Japan Concrete Institute and the Architectural Institute of Japan. His research interests include concrete shear, confined concrete, and seismic design of reinforced and prestressed concrete buildings.*

Shin Okamoto *is a director general at the Building Research Institute, Ministry of Construction, Japan. He received his doctorate degree from Kyoto University in 1987. He is a member of the Japan Concrete Institute and the Architectural Institute of Japan. His research interests include seismic design of reinforced concrete, prestressed concrete, and precast concrete buildings.*

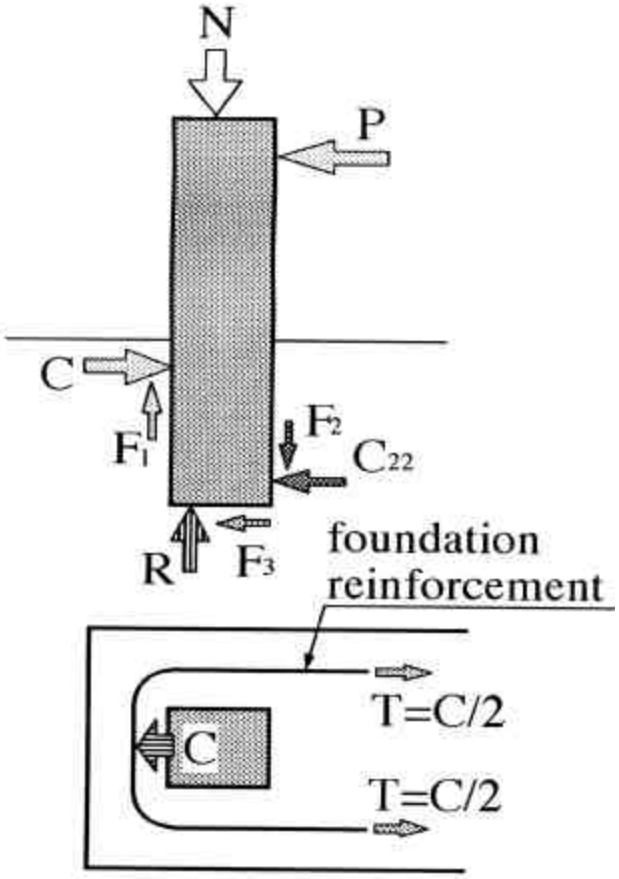

Fig. 1—Stress transmission

It is too complicated to solve the equilibrium equations using only the total model; breaking the total model into two separate models makes it easier to solve them. Each model gives equilibrium equations. From these examples, the equation by which horizontal reaction force will be calculated can be derived.

A building contains perimeter columns and internal columns. On internal columns that have foundation beams on both sides, bearing force *C*, generated by the overturning moment of the column foot in the embedded portions, is transmitted to the compressive zones of the foundation

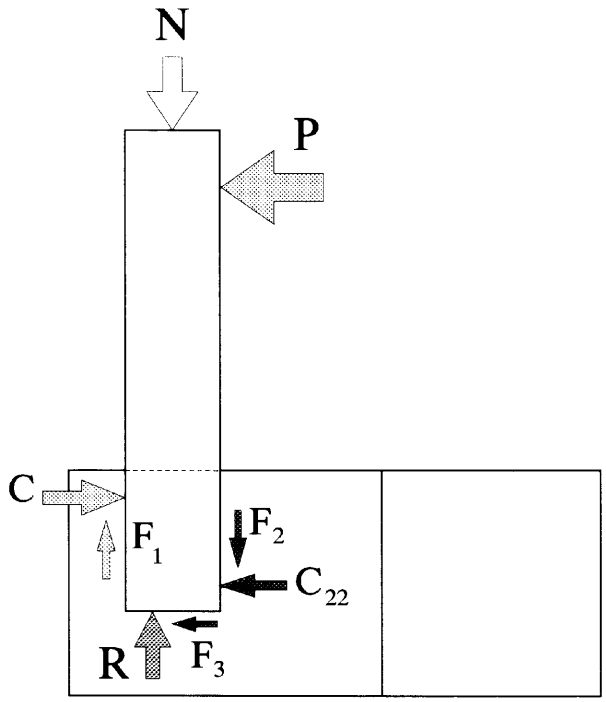

Fig. 2—Total model

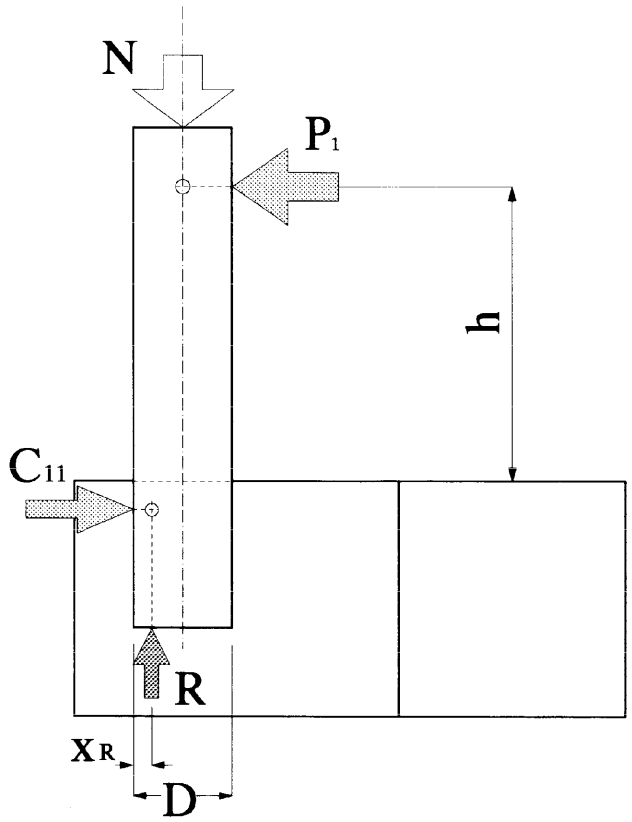

Fig. 3—Model 1

beams via the highly rigid concrete stubs, reducing the tensile force generated in the foundation reinforcement. In this case, the rigidity of the socket base is influenced by the strength of concrete. Structural performance is then improved by using high-strength concrete.

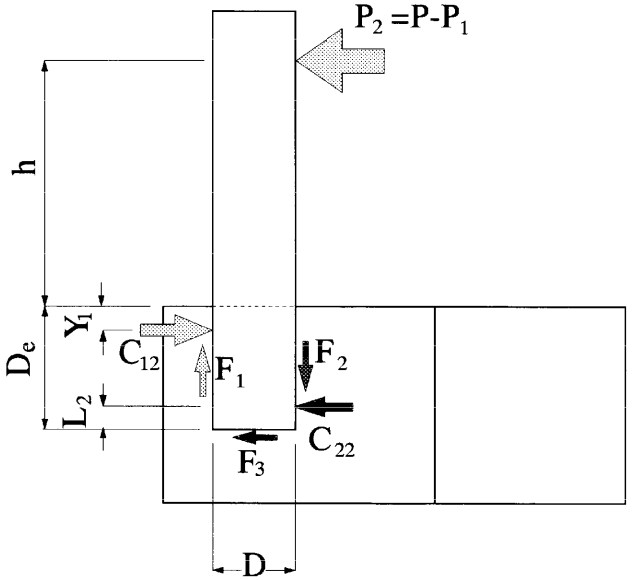

Fig. 4—Model 2

On the other hand, on perimeter columns, bearing force *C* on the side without foundation beams results in the generation of a tensile force in the concrete on the socket walls. This tensile force is resisted by the tensile force in the foundation reinforcement that is anchored into the foundation beams. As the strain in the foundation reinforcement increases, cracks develop in the foundation, leading to a loss of the rigidity in the connection between the columns and the sockets. In perimeter columns, therefore, the structural performance of embedded column bases is greatly influenced by the arrangement detail and amount of foundation reinforcement.

In this study, we predict horizontal reaction force *C* in the socket base by a derived equation and verify its validity. On the perimeter column, as reaction force *C* is resisted by foundation reinforcement, it can be given by the strain of foundation reinforcement. The validity of this theoretical equation is verified by the results of the loading test on the perimeter column model.

Assumptions—Equilibrium equations are formulated under the following assumptions:

1. The tensile resistance of the foundation concrete is ignored.

2. It is assumed that the tensile forces in the foundations are taken only by foundation reinforcement, ignoring the auxiliary reinforcement in the foundations, such as the hoops.

3. The friction forces generated between the faces of the precast column bases and the internal faces of the sockets are considered.

4. Vertical reaction forces equal to the axial forces in the columns are assumed to be acting on the bottom faces of the columns.

5. The total load resisting model (Fig. 2) can be divided into Model 1 (Fig. 3) and Model 2 (Fig. 4).

Formulation of equilibrium equation—First, a position of concrete compressive resultant force at column critical section x_R is calculated for applied load P, assuming plane sections remain plane (see Fig. 5). Fig. 5 shows stress condition at ultimate. This assumption is shown in the Japanese Standard[1] and is customarily used for calculating the nominal strength. The same assumption is also shown in ACI 318-89[2] with different notations. Notation x_R is given as k_2c in ACI 318-89. So, the relationship between concrete compressive stress and concrete strain may be assumed to be rectangular, trapezoidal, parabolic, or any other shape that results in prediction of strength in substantial agreement with the results of comprehensive tests.

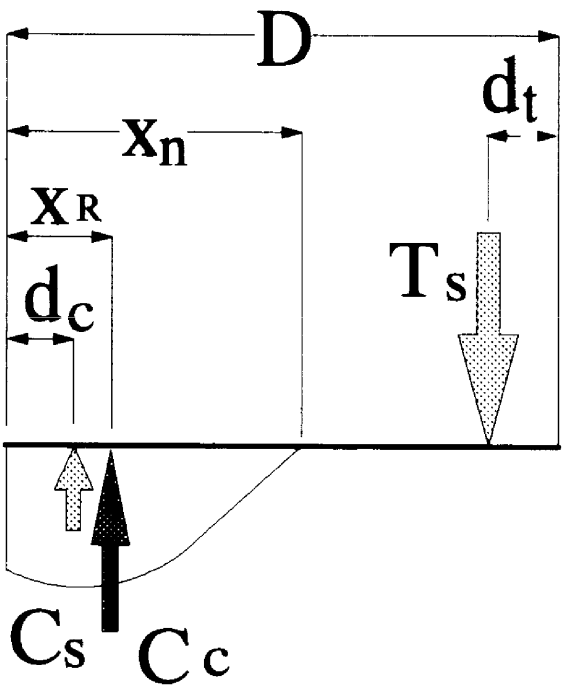

Fig. 5—Stress distribution in column section (C_c = compression force of concrete due to column axial force and overturning moment in column section; C_s = compression force of column reinforcement due to column axial force and overturning moment in column section; D = overall thickness of column; d_c = distance from extreme compression fiber to centroid of compression reinforcement and height of the zone where C_c is acting in concept of AIJ Recom.; d_t = distance from extreme tension fiber to centroid of tension reinforcement and distance from upper end of socket base to point where T_u acts in concept of AIJ Recom.; T_s = tensile force of column reinforcement due to column axial force and overturning moment in column section; x_n = distance from extreme compression fiber to neutral axis; x_R = distance from extreme compression fiber to point where C_s is acting

Then the lateral load carried by Model 1, P_1, and reaction force C_{11} ($= P_1 < P$) are calculated from the equilibrium condition and given as

$$C_{11} = P_1 = \frac{M_1}{h + Y_1} \cong \frac{M_1}{h}\left(\frac{D}{2} - x_R\right) \cdot \frac{N}{h} \qquad (1)$$

where $N = R$ and Y_1 is neglected because Y_1 is small enough compared with h. In Model 2 the sum of the horizontal reaction forces C_{22} and F_3 generated in the socket is noted as C_3 and the position L_3 subject to its action is assumed to be

$$C_3 = C_{22} + F_3, L_3 = (De - 2Y_1)/6 \qquad (2)$$

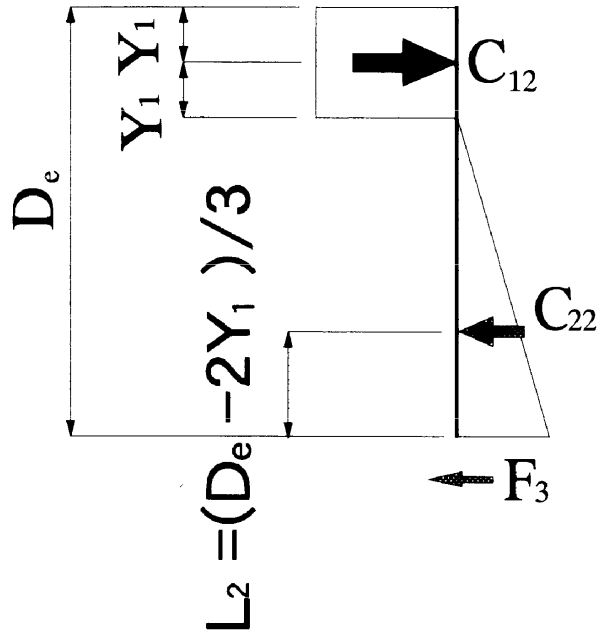

Fig. 6—Stress distribution in embedded portion

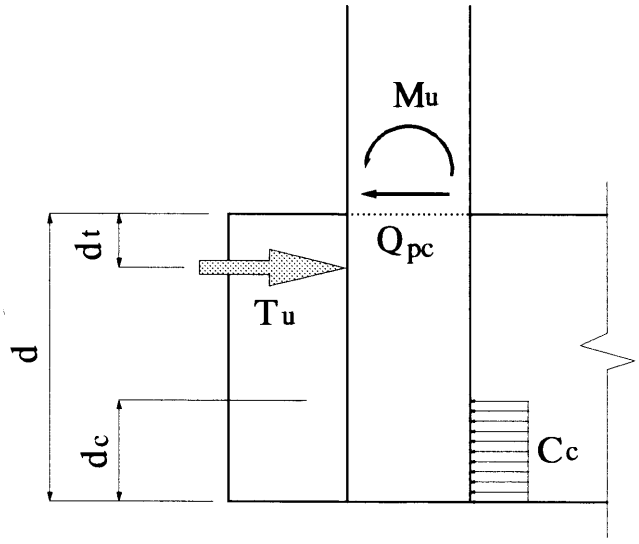

Fig. 7—Concept of AIJ Recom.

Stress distribution in the embedded portion of Model 2 is shown in Fig. 6.

From the equilibrium condition of Model 2, the following equations are obtained.

Moment balance:

$$M_2 + P_2 \cdot De + C_3 \cdot L_3 - C_{12} \cdot (D_e - Y_1) - F_1 \cdot D = 0 \quad (3)$$

Vertical equilibrium:

$$F_1 = F_2 \quad (4)$$

Horizontal equilibrium:

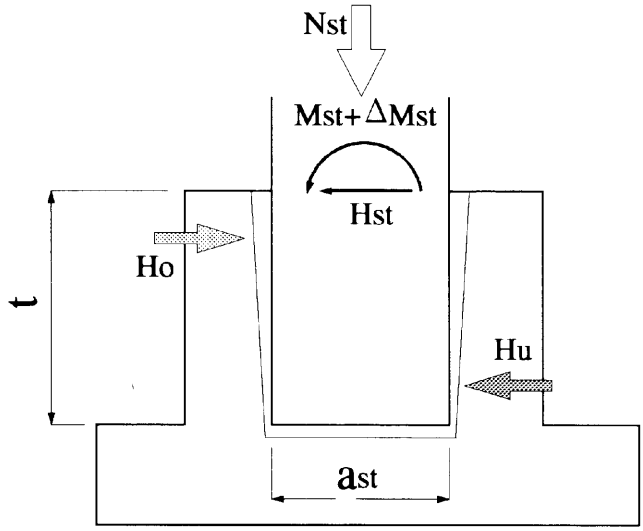

Fig. 8—Concept of DIN 1045

$$C_{12} = P_2 + C_3 \quad (5)$$

where $M_2 = P_2 \cdot h$ (bending moment at column critical section carried by Model 2), while F_1, F_2, and F_3 are the friction forces acting on the surface of the base column in the embedded portion and can be expressed as $F_1 = \mu_1 \cdot C_{12}$, $F_2 = \mu_2 \cdot C_{22}$.

Total reaction C is obtained as

$$C = C_{11} + C_{12} \quad (6)$$

Reaction C shall be transmitted to the foundation reinforcement (see Fig. 1). From Eq. (3) through (6), the theoretical equation for calculation of C, Eq. (7), can be derived

$$C = \frac{1}{L_0 - L_3 + \mu_1 \cdot D} \cdot \left\{ M + (D_e - L_3) \cdot Q + e_c \cdot [(\mu_1 - \alpha) \cdot D - Y_1] \cdot \frac{N}{\alpha} \right\} \quad (7)$$

where $M = P \cdot h$, $Q = P$, $\alpha = \frac{h}{D}$, $e_c = \frac{D}{2} - x_R$

Equations given in the AIJ Recom. are shown below for reference (Fig. 7)

$$M_u' = Tu \cdot \left(\frac{d}{2} - d_t \right) + C_c \cdot \left(\frac{d}{2} - \frac{d_c}{2} \right) \quad (8)$$

where

M_u' = ultimate bending strength of base > M_u

M_u = ultimate bending strength of column

$T_u = Q_{pc} + C_c$

Replacing M_u' by M_u, T_u can be calculated as

$$T_u = \frac{1}{d - d_t - d_c/2} \cdot \left\{ M_u + \frac{Q_{pc}}{2} \cdot (d - d_c) \right\} \quad (9)$$

Equations for H_0 (Fig. 8) given in DIN 1045 are shown below, with a rough finish on the column face and socket inner face and with a smooth one, respectively

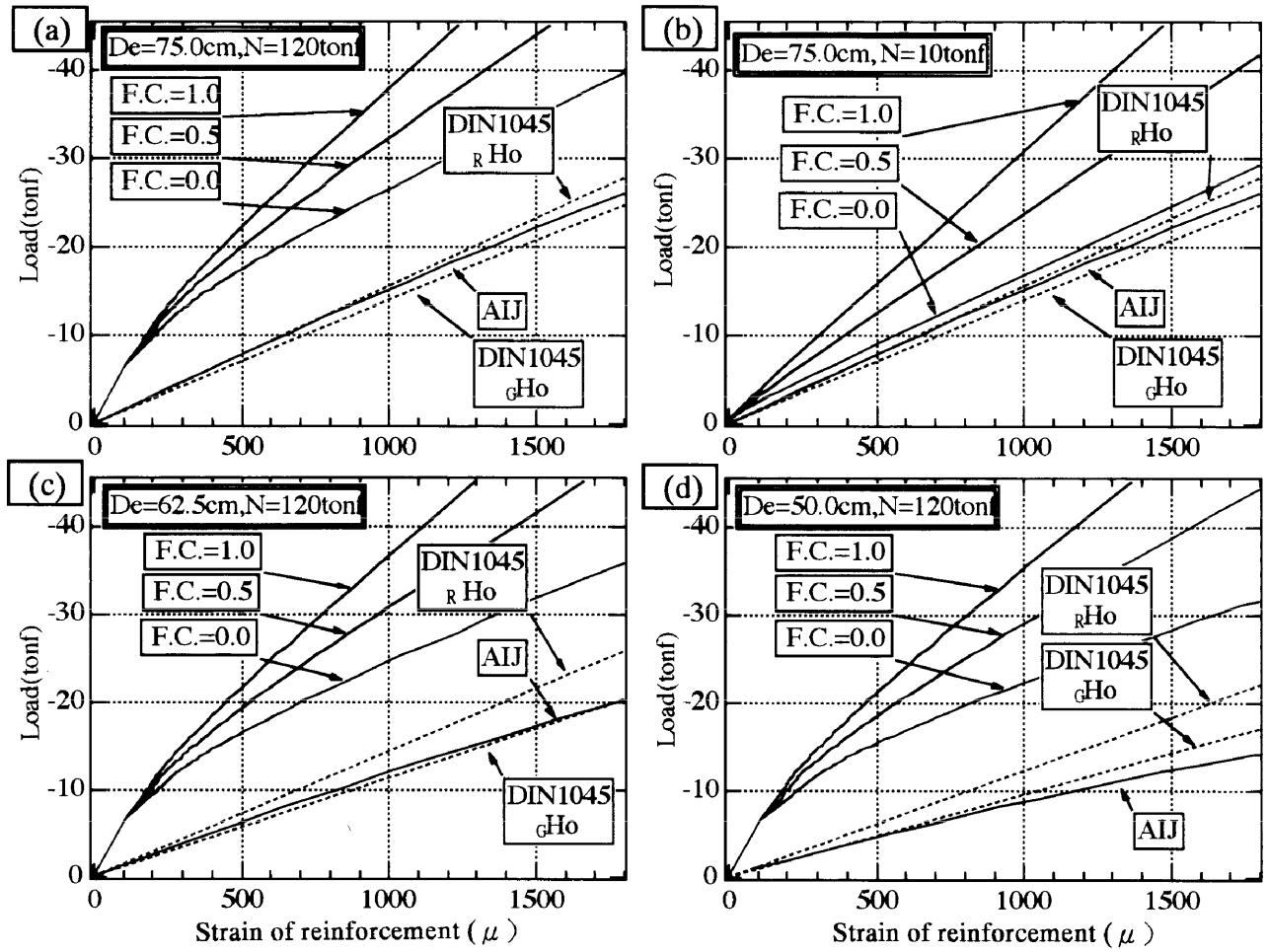

Fig. 9—Theoretical calculation results: load-strain curves for foundation reinforcement (AIJ = AIJ Recom., F. C. = friction coefficient; 1.0 tonf = 9807 N)

$$ {}_{R}H_0 = \frac{6}{5} \cdot \frac{M_{st} + \Delta M_{st}}{t} + \frac{6}{5} \cdot H_{st} \quad (10) $$

$$ {}_{G}H_0 = \frac{3}{2} \cdot \frac{M_{st} + \Delta M_{st}}{t} + \frac{5}{4} \cdot H_{st} \quad (11) $$

where

M_{st} = moment caused by horizontal force-acting column

ΔM_{st} = moment caused by eccentric column axial force

Calculation results—Theoretically predicted load-foundation reinforcement strain relations are indicated in Fig. 9. Theoretical calculations were conducted on model specimens that had a column section width of 40 cm, column section height of 50 cm, height of loading point 150 cm, and eight 22-mm-diameter deformed bars as foundation reinforcement (see Fig. 10). Variables in the calculation were the embedment length, column axial force, and friction coefficient. The results obtained with the equations given in the AIJ Recom. and DIN 1045 agreed closely with each other. In comparison, the curves obtained with the theoretical equation proposed in this study indicate smaller strains at the same loads, the strain becoming smaller as the friction coefficient increases.

Although the curves obtained with the theoretical equation proposed in this study approach those obtained with the equations in the AIJ Recom. and DIN 1045 when the friction coefficient is zero, they show significant difference from the latter when the friction coefficient was increased to 0.5 and 1.0.

The theoretical equation expresses the fact that the force generated inside the socket becomes smaller as the column axial force or the friction coefficient increases.

In this theoretical approach, friction coefficient μ should be given. Therefore, a test was carried out to determine the appropriate friction coefficients as well as to confirm the validity of the modeling.

TESTS

Specimens

The properties of the materials used in the preparation of the specimens and the parameters of the specimens are given in Tables 1 and 2; the specimens are illustrated in Fig. 10.

On Types 18, 19, 22, and 23, shear keys (Fig. 11) were formed on all four faces on both the columns and the socket walls. Their embedment depths were 75, 62.5, and 50 cm, respectively. Types 10, 15, 16, and 17 are specimens without shear keys. In these specimens, the columns were placed in steel forms and the internal faces of the sockets in wooden forms, with no surface finishing after form removal. Their embedment depths were 75, 62.5, and 50 cm, respectively.

Specimens were assembled by inserting the columns into the sockets in the foundations and filling gaps of 4 cm on

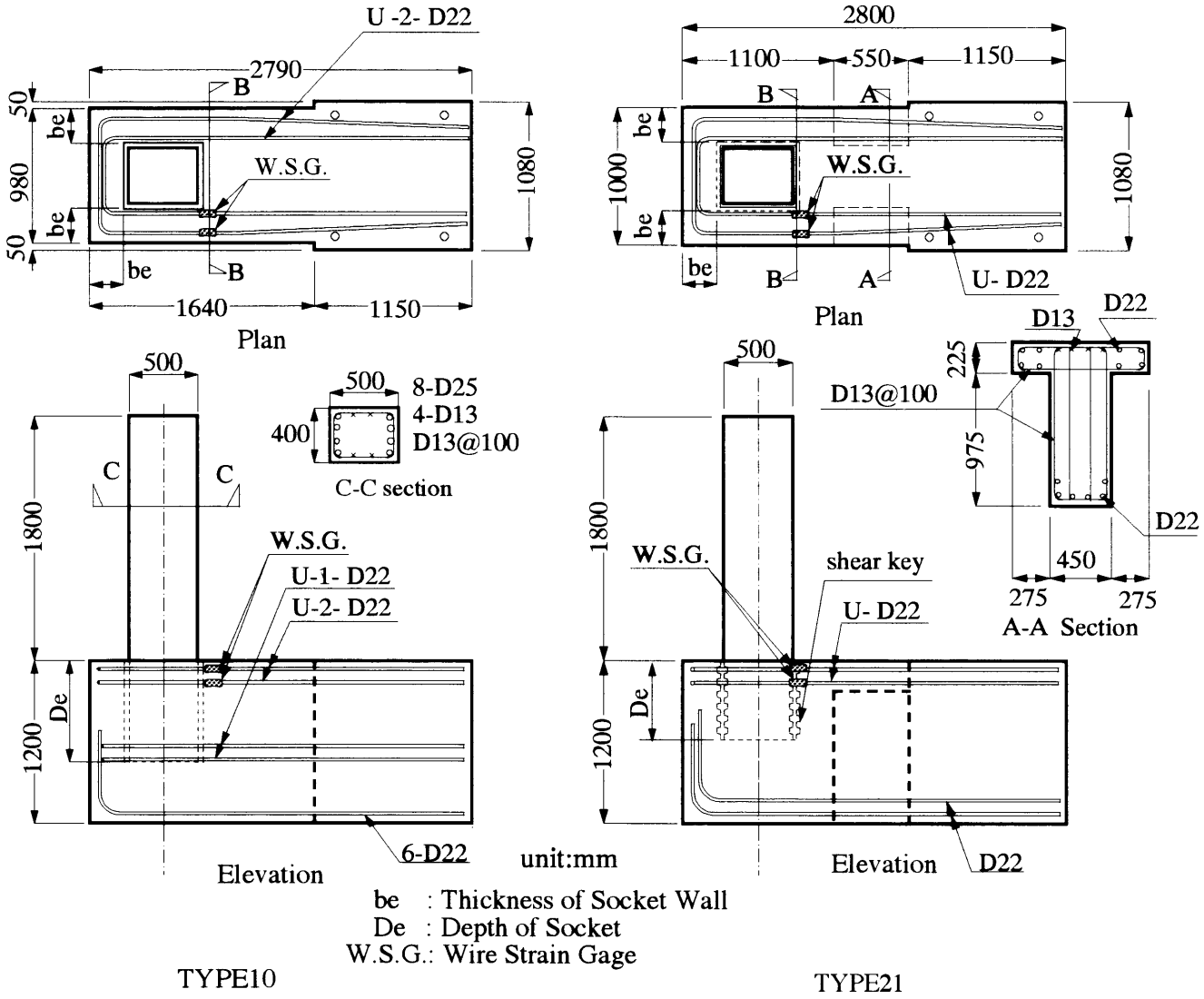

Fig. 10—Specimen

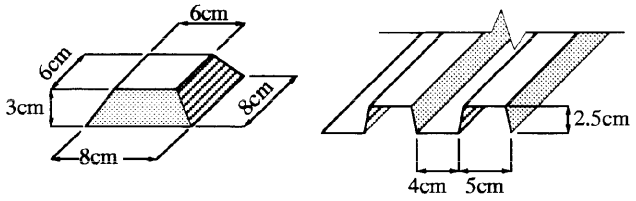

Fig. 11—Shear key

each side with nonshrinking concrete with a strength of Fc = 400 kgf/cm^2. In Types 21, 22, and 23 with steel shear key form and smaller gaps of 25 mm, nonshrinking mortar with a strength of Fc = 400 kgf/cm^2 was used. For the foundation reinforcement, four U-shaped D22 bars were positioned around the column and their ends were anchored to the stubs for fixing the specimen.

In Types 21, 22, and 23, T-shaped beams with small cross sections, as shown in Fig. 10 (Section A-A), were used for the foundation beams and the foundation reinforcement was anchored to the stubs for fixing the specimens through flanges. The auxiliary reinforcement (vertical bars and hoops in socket, stirrups for foundation beams, stirrups for stubs, etc.) is omitted from the illustration.

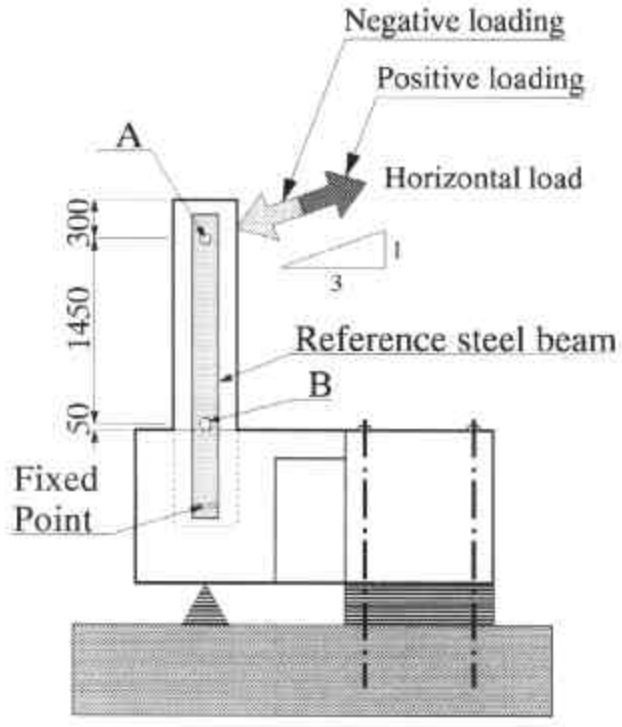

Fig. 12—Loading method

Table 1—Concrete

	Concrete				Parameter	
	Basement		Column			
Specimen	${}_c\sigma_b$, kgf/cm^2	E, kgf/cm^2	${}_c\sigma_b$, kgf/cm^2	E, kgf/cm^2	D_e, cm	Shear key
Type 10	262	249,000	389	287,000	75.0	Without
Type 15	189	187,000	411	290,000	75.0	Without
Type 16	193	185,000	431	306,000	62.5	Without
Type 17	187	182,000	403	281,000	50.0	Without
Type 18	203	212,000	440	309,000	75.0	With
Type 21	281	255,000	421	302,000	62.5	With
Type 22	168	173,000	402	290,000	62.5	With
Type 23	161	165,000	449	219,000	50.0	With

Note: 1.0 kgf/cm^2 = 0.0009807 Pa.

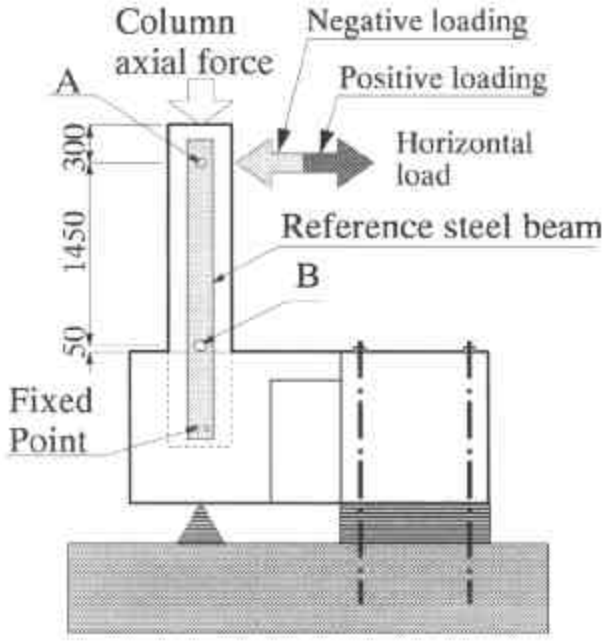

Fig. 13—Loading method (Type 22)

Table 2—Reinforcement

Diameter, mm	σ_v, kgf/cm^2	σ_b, kgf/cm^2	E, kgf/cm^2	Group
D13	3140	4720	1,940,000	A
D13	3420	5280	1,870,000	B
D22	3820	5730	1,850,000	A
D22	3920	5740	1,940,000	B
D25	3860	5370	1,880,000	A
D25	4010	5780	1,940,000	B

Note: Group A: Type 15, 16, 17, 18; Group B: Type 10, 21, 22, 23.
1.0 kgf/cm^2 = 0.0009807 Pa.

Table 3—Applied vertical load

Specimen	Vertical load
Type 15	10.0
Type 22	0.0
Others	120.0

Note: 1.0 tonf = 9807 N

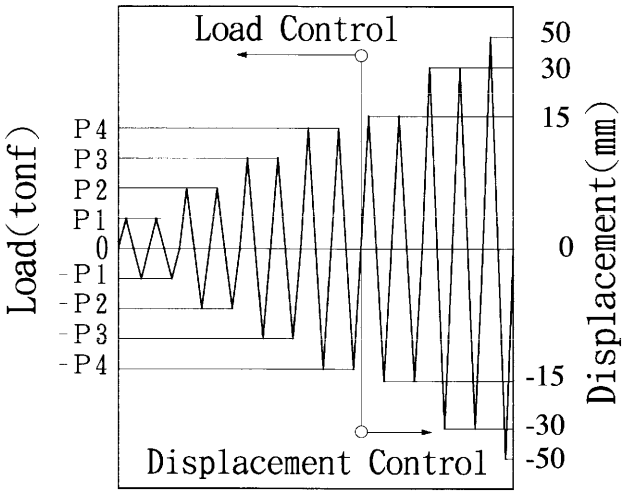

Fig. 14—Loading pattern (1.0 tonf = 9807 N)

Loading and measurement methods

The loading method is illustrated in Fig. 12 and 13. The applied vertical loads N are shown in Table 3. On Types 10, 16, 17, 18, 21, and 23, a constant column axial force N of 120 tonf was applied at Point A. On Type 15, the column axial force of N, 10 tonf, was applied. On Type 22, there is no vertical load.

At the same time, alternating positive and negative horizontal loads P were applied. The horizontal loading pattern is shown in Fig. 14. On Type 22, the horizontal jack was positioned at an angle (see Fig. 13) so that one-third of the horizontal load would act as a column axial force; in other words, an alternating tension and compression column axial force proportional to the horizontal load was applied to Type 22.

Horizontal displacement was measured at Point A and the rotational and horizontal displacements were measured at Point B with reference to the post fixed to the side face of a socket wall. Strain in the foundation reinforcement was measured with the wire strain gages attached at position B-B, shown in Fig. 10.

The applied loads in the test are in Table 4. The strength of column shown in Table 5 is calculated according to the reference literature.[3] Loading was controlled by the load in the first half of the test and by displacement in the following postyield range of deformation.

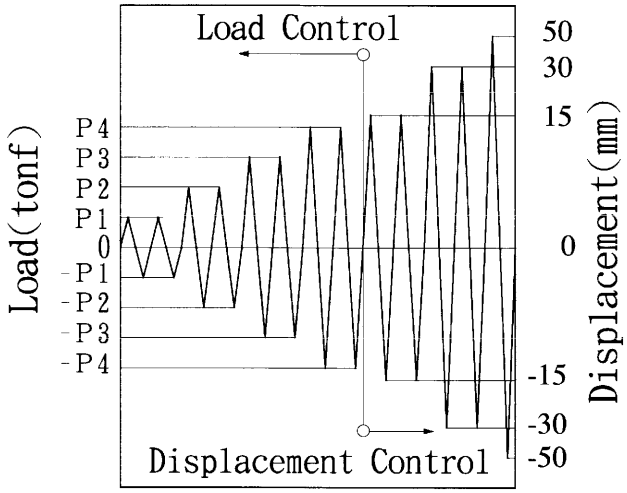

Fig. 14—Loading pattern (1.0 tonf = 9807 N)

Table 4—Applied horizontal load in test

Specimen	P1	P2	P3	P4
Type 15, 22	3.0	5.0	15.0	18.0
Others	6.0	12.0	20.0	33.0

Note: 1.0 tonf = 9807 N

Test results

Envelopes for the load (P)-displacement (δt) curves for the tops of the columns (Point A) are shown in Fig. 15. With the exception of Types 15 and 22, with their small column axial forces, all specimens showed more or less the same curves under positive loading. The curves for Type 15 in Fig. 15(a) and Type 22 in Fig. 15(b) also agree with each other.

Under negative loading, while Type 10 in Fig. 15(c) and Types 18, 21, and 23 in Fig. 15(d) give more or less the same curves, Types 16 and 17 in Fig. 15(c) show small rigidity beyond P = -28 tonf. It can be said that horizontal displacement at the column foot due to tensile strain of the foundation reinforcement results in rotation in the embedded portion. Smaller embedment depth results in larger rotation if the horizontal displacement of the column foot is the same. On Types 16 and 17, embedment depths are smaller than the one on Type 10 in Fig. 15(c); Type 16 and 17 show small rigidity. While Type 15 in Fig. 15(c) and Type 22 in Fig. 15(d) show similar curves, the member yield point is clearer for Type 22 than for Type 15.

With Type 16 in Fig. 15(d), the predicted strength given in Table 5 is reached when δ_t = approximately 30 mm (R = 1/70 radian), indicating a large deformation.

Type 17 in Fig. 15(d) did not reach the predicted strength given in Table 5 due to small embedment depth, but showed an almost constant carrying capacity of 32 tonf in postyield range.

From experimental observation, this phenomenon could be estimated due to the progress of inelastic deformation of the compressed concrete while the strain of foundation reinforcement was kept constant in elastic range, resulting in a degradation of the rigidity of column base against horizontal load.

Table 5—Predicted horizontal loads by column

Horizontal load	Column axial force	
	120.0 tonf	10.0 tonf
At flexural cracking load	10.7	4.6
At long-term permissible load	16.9	15.4
At flexural shear cracking load	21.9	13.3
At ultimate bending strength	37.6	22.2

Note: 1.0 tonf = 9807 N

With Type 23 in Fig. 15(d), provided with shear keys, though with the same embedment depth of 50 cm (column depth D x 1.0) as Type 17 in Fig. 15(c), the predicted strength of column given in Table 5 has been reached, and the load-displacement curve approximates that of Type 18 in Fig. 15(d) with an embedment depth of 75 cm (column depth D x 1.5). It is to be concluded that the addition of the shear keys allows the larger friction forces at the column-socket interfaces, including column side faces, leading to a decrease of reaction C and an improvement in the rigidity of the column base.

COMPARISON OF CALCULATION AND TEST RESULTS

Load-strain curves for foundation reinforcement are shown in Fig. 16 and 17. The results for Types 10 and 18 are given in Fig. 16(a). After horizontal force P exceeds -18 tonf, the gradient of the curve becomes gentler for Type 18 and the strain is greater than in Type 10. The test results for Type 10 approximate the calculation results obtained with a friction coefficient of 1.0 and the test results for Type 18 approximate those obtained with a friction coefficient of 0.5.

Results for Type 16 are given in Fig. 16(b). Here, there is a large discrepancy between the calculation and test values in the low-load region. This is thought to be due to the behavior of the foundation cross section as a composite concrete-reinforcement body, with the two cooperating in resisting the force while the crack widths remain small. In other words, Assumption 1, in which tensile resistance of foundation concrete is ignored, does not hold in the low-load region and only comes into operation as the load increases. The curve for the test results is found between the curves obtained with friction coefficients of 0.5 and 1.0 as one approaches the ultimate load.

Results for Types 16 and 21 are given in Fig. 17(a). The degradation of the rigidity begins earlier in Type 16. The curves for the two specimens show similar gradients, with Type 16 showing a greater strain throughout. Both types give curves similar to the calculation results obtained with a friction coefficient of 1.0.

The results for Type 22, with an embedment depth (De) of 62.5 cm subject to a column axial force (N) corresponding to one-third of the horizontal force (P/3), are given in Fig. 17(b). The curve is similar to that for Type 15. There is a large discrepancy between the calculation and test values in the low-load region and the curve for the test results is found between the curves obtained with friction coefficients of 0.5 and 1.0 as one approaches the ultimate load.

Results for Types 17 and 23 are given in Fig. 17(c). The degradation of the rigidity begins earlier in Type 17. Tangent

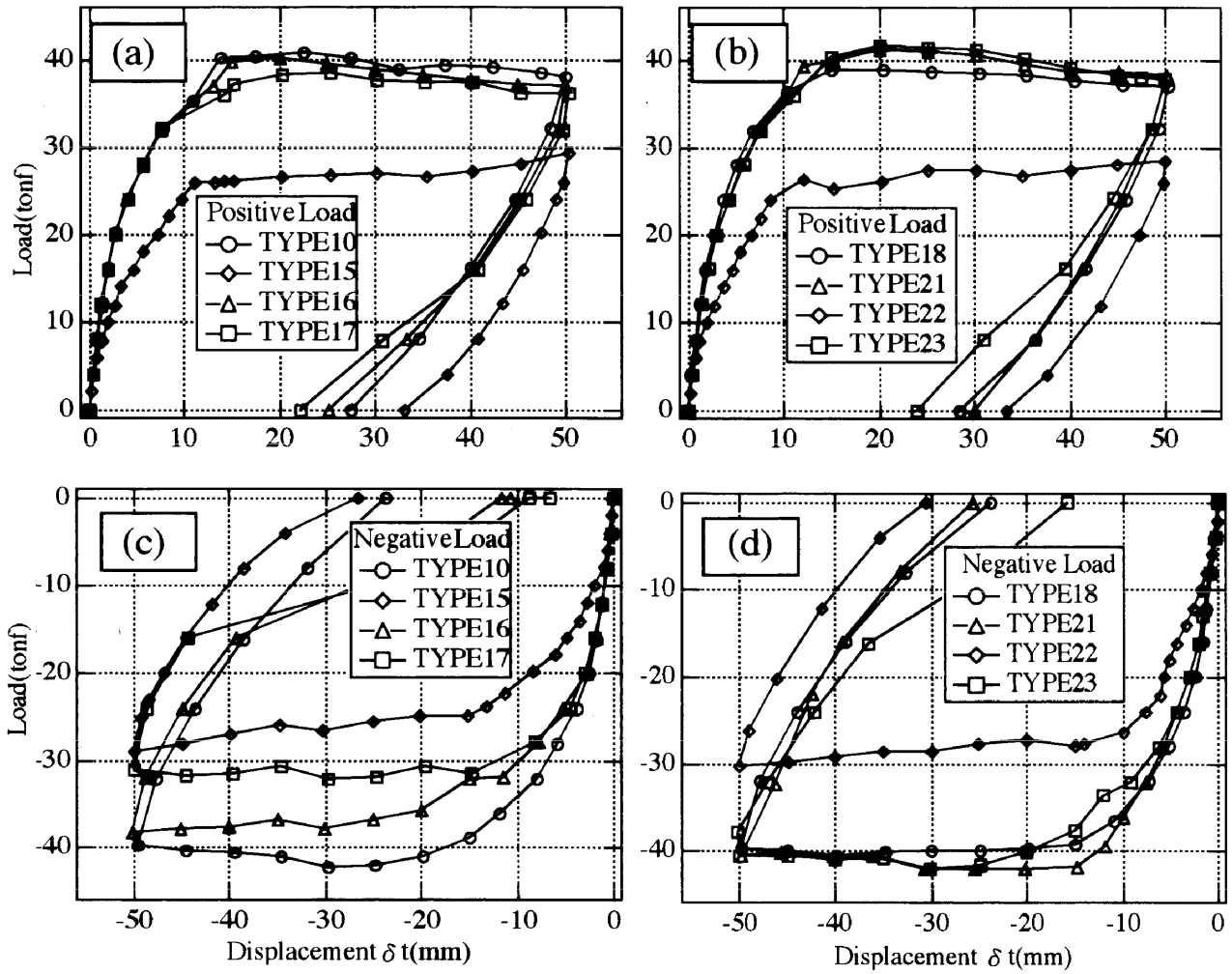

Fig. 15—Horizontal load (P)-displacement (δ_t) curves (1.0 tonf = 9807 N)

stiffness for Type 23 is decreasing gradually up to the maximum load. On the other hand, the curve for Type 17 has a bilinear shape with a sharp bend at load P = -8 tonf, reaching the same level as Type 23 at P = -30 tonf. Since, as mentioned previously, the degradation of the rigidity prevented increases in the horizontal load on Type 17 beyond P = -32 tonf, comparison cannot be made beyond this point. Up to P = -30 tonf, the curve for Type 23 approximates that obtained with a friction coefficient of 1.0. Beyond this, the strain exceeds that obtained with a friction coefficient of 1.0 to come gradually close to that obtained with a friction coefficient of 0.5.

Findings from the observation of strain responses of foundation reinforcement are: 1) degradation of rigidity begins earlier in specimens without shear keys; 2) load-strain curves come close to the predicted values near the ultimate load when friction coefficients of 0.5 to 1.0 are used; 3) specimens with an embedment depth of 1.5D and those with an embedment depth of 1.25D provided with shear keys give results similar to those obtained in calculation with a friction coefficient of 1.0; and 4) specimens with an embedment depth of 1.0D provided with shear keys give results similar to those obtained in calculation with a friction coefficient of 0.5.

CONCLUSION

The following conclusions were drawn from the results of the theoretical calculations and tests conducted by the authors. The highlights of structural performances are shown in Table 6.

1. If the embedment depth is 1.5D or more, the column base is regarded as being in a rigid connection even without shear keys.

2. The resultant force transmission performance of the column bases can be improved by the addition of shear keys. Socket base connections with embedment depths of 1.0D or more when provided with shear keys give results similar to those with an embedment depth of 1.5D and can reach the ultimate strength of the columns.

3. Socket base connections without shear keys do not have enough rigidity when an embedment depth is less than 1.25D, although in the case of an embedment depth of 1.25D a column can reach its ultimate flexural strength in large deflective situations, such as a rotation angle of 1/70.

4. The friction coefficients in Table 7 according to embedment depth and shear key are recommended. The value of 1.0 is recommended for the friction coefficient for the socket when the embedment depth is 1.5D or more without shear keys or when the embedment depth is 1.25D or more with shear keys, while the value of 0.5 is recommended when the embedment depth is 1.0D with shear keys.

5. Commencement of degradation of rigidity can be delayed by providing specimens with shear keys.

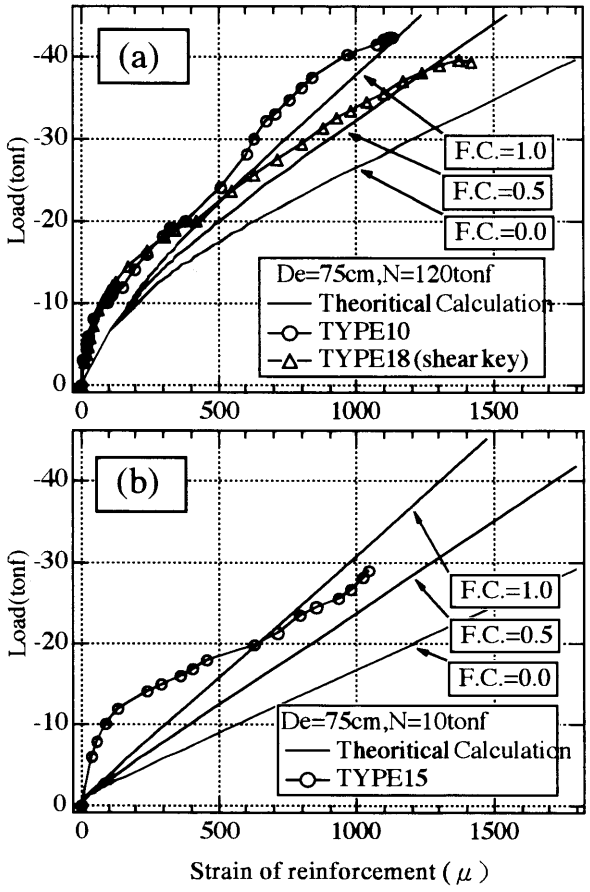

Fig. 16—Load-strain curves for foundation reinforcement[1] (1.0 tonf = 9807 N)

Table 6—Structural performance

Embedded depth	Shear key	Strength	Displace-ment	Structural perfor-mance	Specimen
1.0D (50 cm)	Without	Not enough	Large	No good	Type 17
1.0D (50 cm)	With	Enough	Compara-bly large	Good	Type 23
1.25D (62.5 cm)	Without	Enough	Large	Moder-ately good	Type 16
1.25D (62.5 cm)	With	Enough	Small	Good	Type 21 Type 22
1.5D (75 cm)	Without	Enough	Small	Good	Type 10 Type 15
1.5D (75 cm)	With	Enough	Small	Good	Type 18

Table 7—Recommended friction coefficient

Friction coefficient	Embedded depth	Shear key
1.0	1.5D or more	Without
1.0	1.25D or more	With
0.5	1.0D	With

6. The theoretical equation proposed previously gives results that are closer to the test values for embedded precast

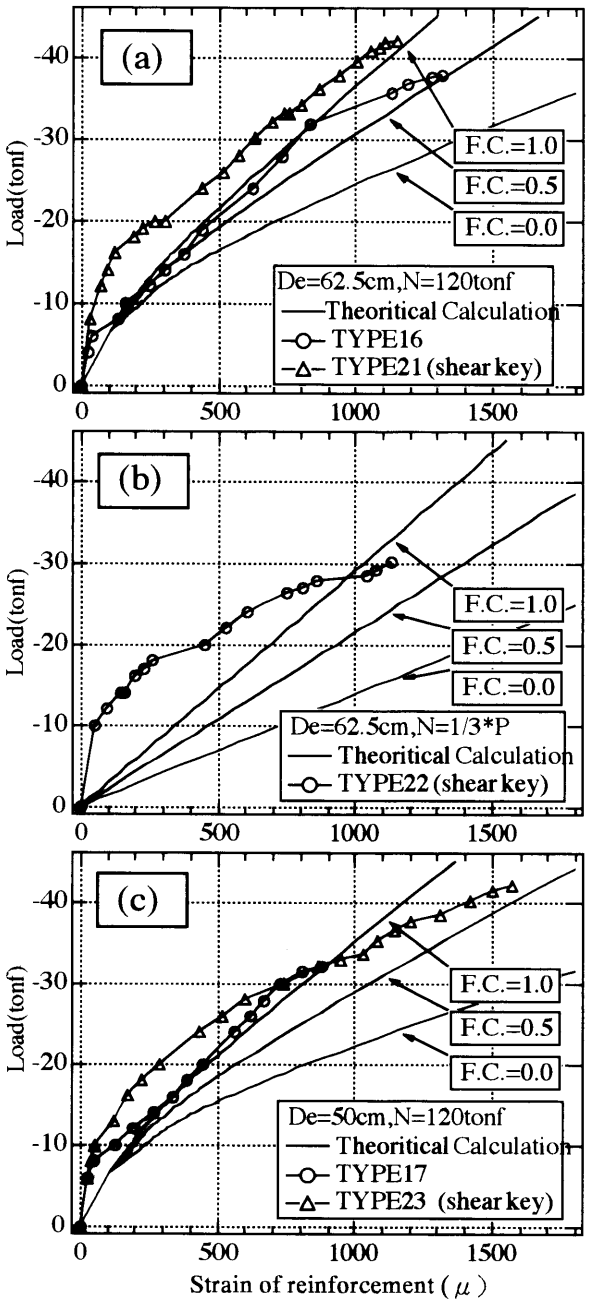

Fig. 17—Load-strain curves for foundation reinforcement[2] (1.0 tonf = 9807 N)

reinforced concrete columns than the equations in the AIJ Recom. and DIN 1045. The load-strain curves for the foundation reinforcement come close to the test values near the ultimate load when friction coefficients of 0.5 to 1.0 are used.

NOTATION

a_{st} = overall thickness of column in concept of DIN 1045
b_e = thickness of socket wall
C = compression force of column reinforcement due to column axial force and overturning moment in column section
C_c = compression force of concrete due to column axial force and overturning moment in column section
C = resultant reaction force due to lateral load
C_3 = resultant reaction force due to lateral load
C_{12} = resultant reaction force due to lateral load
C_{22} = resultant reaction force due to lateral load
d = depth of socket in concept of AIJ Recom.

d_c = height of zone where Cc is acting in concept of AIJ Recom.
d_e = distance from extreme compression fiber to centroid of compression reinforcement
d_t = distance from upper end of socket base to point where Tu is acting in concept of AIJ Recom.
d_t = distance from extreme tension giver to centroid of tension reinforcement
D = overall thickness of column
D_e = depth of socket
E = modulus of elasticity of concrete or reinforcement
FC = friction coefficient
F_1 = friction force generated between surface of precast column faces and internal faces of socket
F_2 = friction force generated between surface of precast column faces and internal faces of socket
F_3 = friction force generated between surface of precast column faces and internal faces of socket
${}_GH_0$ = horizontal reaction force with smooth finish on column surfgace in concept of DIN 1045
h = height of point where P is acting from upper end of socket base
H_{st} = transmitted horizontal shear force in concept on DIN 1045
H_u = horizontal reaction force in concept of DIN 1045
H_0 = horizontal reaction force with rough finish on column surface in concept of DIN 1045
L_0 = distance from point where C11 is acting to one where C is acting
L_2 = distance from point where C12 is acting to one where C22 is acting
L_3 = distance from point where C12 is acting to one where C is acting
M_{st} = transmitted overturning moment at column base in concept of DIN 1045
M_u = transmitted overturning moment at column base in concept of AIJ Recom.
N = column axial force
N_{st} = column axial force in concept of DIN 1045
P = lateral load at top of column of specimen
P_1 = lateral load at top of column of specimen
P_2 = lateral load at top of column of specimen
Q_{pc} = transmitted horizontal shear force in concept of AIJ Recom.
R = resultant reaction force due to column axial force
${}_RH_0$ = horizontal reaction force in concept of DIN 1045
t = depth of socket in concept of DIN 1045
T = resultant reaction force of foundation reinforcement due to lateral load
T = tensile force of column reinforcement due to column axial force and overturning moment in column section
T_u = resisting force of foundation reinforcement in concept of AIJ Recom.
x_n = distance from extreme compression fiber to neutral axis
x_R = distance form extreme compression fiber to point where Cs is acting
Y_1 = distance from upper end of socker base to point where Tu is acting
ΔM_{st} = increment of overturning moment at column base in concept of DIN 1045
${}_c\sigma_b$ = compressive strength of concrete
σ_b = tensile strength of reinforcement
σ_y = yield strength of reinforcement

REFERENCES

1. "Standard for Calculation of Reinforced Concrete Structures," Architectural Institute of Japan, 1988, pp. 602.

2. ACI Committee 318, "Building Code Requirements for Reinforced Concrete and Commentary (ACI 318-89/ACI 318R-89)," American Concrete Institute, Detroit, 1989, pp. 6-1 to 6-11.

3. "Data for Ultimate Strength of Reinforced Concrete Structures," Architectural Institute of Japan, 1990, pp. 70-71.

4. "Recommendations for the Design and Fabrication of Tubular Structures in Steel," Architectural Institute of Japan, 1990, pp. 237-242.

5. "Examples for Calculation in Accordance with DIN 1045," Deutscher Beton-Verein E.V., 1981, pp. 204-224.